Cancer Letters 461 (2019) 10–20

Contents lists available at ScienceDirect

Cancer Letters

journal homepage: www.elsevier.com/locate/canlet

Original Articles

Interference with the bromodomain epigenome readers drives p21 expression and tumor senescence

Liana P. Webber[a,b], Veronica Q. Yujra[a,c], Pablo A. Vargas[d], Manoela D. Martins[b], Cristiane H. Squarize[a,e], Rogerio M. Castilho[a,e,*]

[a] Laboratory of Epithelial Biology, Department of Periodontics and Oral Medicine, University of Michigan, School of Dentistry, Ann Arbor, MI, 48109, USA
[b] Department of Oral Pathology, School of Dentistry, Federal University of the Rio Grande do Sul, Porto Alegre, RS, 90035-004, Brazil
[c] Department of Pathology, Federal University of São Paulo, Sao Paulo, SP, 04023-062, Brazil
[d] Oral Diagnosis Department, Piracicaba Dental School, University of Campinas, Piracicaba, SP, 13414-903, Brazil
[e] University of Michigan Comprehensive Cancer Center, Ann Arbor, MI, 48109, USA

ARTICLE INFO

Keywords:
Tumor suppression
Xenograft
Cancer stem cell
Head and neck cancer
Senescence

ABSTRACT

Head and neck cancer (HNSCC) are one of the most common solid malignancies of the world, being responsible for over 350,000 deaths every year. Much of the complications in managing and treating HNSCC advent from the complex genetic and epigenetic landscape of the disease. Emerging information has shown promising results in targeting BRD4, an epigenetic regulator bromodomain that functions as a scaffold for transcription factors at promoters and super-enhancers. Here we show that by disrupting the interaction between BRD4 and histones using the bromodomain inhibitor JQ1, HNSCC cells undergo cell growth arrest followed by cellular senescence. Mechanistically, JQ1 negatively impacted the phosphorylation levels of SIRT1 along with the acetylation levels of mutant p53 (active). *In vivo* administration of JQ1 resulted in disruption of HNSCC growth along with the activation of cellular senescence, observed by the accumulation of DNA double-strand breaks, $p16^{ink4}$, accumulation of senescence-associated beta-galactosidase, and loss of phosphorylated $Sirt1^{ser47}$. Furthermore, we also demonstrate that JQ1 was efficient in reducing the population of cancer stem cells from HNSCC xenografts.

1. Introduction

Head and neck cancers are the sixth most common cancer worldwide, with approximately more than half a million new cases diagnosed annually, and over than 350,000 deaths every year [1]. The process of cellular transformation and tumor progression is a result of multiple steps that involve many genetic and epigenetic modifications [2].

The epigenome is the combination of chemicals and proteins capable of directly attaching to the DNA (genome) and modify gene expression. Locally, cells can differentially use the information from the genome by activating and deactivating gene expression accordingly to the given needs of a tissue. The modifications to the DNA resulting in changes of gene expression are called “marks” and can have a transitory effect or be persistent and capable of passing down through generations. Histone acetylation and DNA methylation are marks that modulate gene expression. The epigenome is continuously changing during the lifespan of an organism in response to environmental factors.

Our interest relies on epigenetic events driven by histone modifications. Histone modifications are transient and fast-occurring events as we have previously characterized during tumor acquisition of chemoresistance [3]. We have also shown that histone modifications have a direct impact on the fate of stem cells-like cancer cells and in the sensitivity of tumor cells to chemotherapy [4–7]. However, the mechanism by which histone modifications can modify tumor fate is not fully understood. Here, we decided to explore the role of the bromodomain and extra-terminal (BET) family containing protein 4 (BRD4) in the biology of HNSCC. BET is a family of proteins which recognize acetylated histone through bromodomains (BD) thereby playing a crucial role in genetic expression. BET family includes BRD2, BRD3, BRD4, and BRDT.

BRD4 function as chaperons to facilitate transcription through histone H4. Also, BRD4 plays an essential role in the colony formation of embryonic stem cells (ESC), along with the self-renewal ability of ESC and expression of associated pluripotency genes [8–10]. Indeed, expression levels of BRD4 are found reduced during cellular differentiation of embryonic stem cells [11]. Here, we explored the effects of BRD4 histone H4 binding displacement using the BET inhibitor JQ1. JQ1 is a small molecule with low nanomolar binding potency against all

* Corresponding author. Laboratory of Epithelial Biology, University of Michigan, 1011 N University Ave, Room 2029c, Ann Arbor, MI, 48109-1078, USA.
E-mail address: rcastilh@umich.edu (R.M. Castilho).

https://doi.org/10.1016/j.canlet.2019.06.019
Received 18 February 2019; Received in revised form 26 June 2019; Accepted 27 June 2019

BET subfamily members, and primarily targeting BRD4 [12,13].

We show that administration of JQ1 to head and neck tumor cells disrupt their ability to form colonies. Remarkably, BRD4 inhibition also triggered cellular senescence on head and neck tumor cells along with downregulation of SIRT1, a NAD-dependent deacetylase known to be associated with longevity and enhanced survival of human stem cells [14]. Most exciting, we found that disruption of BRD4/histone H4 binding reduced the number of stem cells-like cancer cells, a subpopulation of tumor cells capable of evading chemo and radiotherapy and frequently involved in tumor regrowth. All in all, we observed that pharmacological displacement of the BRD4-histone H4 binding halts head and neck tumor growth while inducing tumor senescence.

2. Materials and methods

2.1. Cell lines and administration of JQ1

HNSCC cell lines HN6, HN12, and HN13 were maintained in a 5% CO_2 humified incubator at 37 °C Vehicle group received DMSO, and JQ1 group received a final concentration of 1 μM (Cayman Chemical, Ann Arbor, MI, USA).

2.2. Human tissue specimens

Human HNSCC tissue samples (n = 19) and normal human oral mucosa (NOM) tissue samples (n = 6) were retrieved from the archives of the Laboratory of Pathology of the Porto Alegre University Hospital in Brazil (Human Research Ethics Committee approval: 49942215.2.0000.5327).

2.3. Tissue microarray and BRD4 expression

HNSCC tumor samples were microscopic reviewed by two pathologists, and area of interest was select according to the tumor-specific reference slide stained with hematoxylin and eosin (Beecher Instruments, Silver Spring, MD). Tissue microarray (TMA) was prepared using two punctured tissues per tumor sample retrieved from a 1.0-mm needle.

2.4. Immunofluorescence and Immunohistochemistry

Tumor cell lines were seeded on glass coverslips in 6-well plates and fixed with paraformaldehyde at room temperature for 20 min. Paraffin-embedded tumor samples and cultured cells were incubated with anti-BRD4, anti-p-SIRT-1, anti-acetyl-Histone H4 (Lys5,8,12,16), anti-γ-$H2AX^{ser129}$, and anti-ALDH1A1 following by secondary antibody conjugated with Alexa Fluor 488 or 568. For immunohistochemistry, cells and tissue samples were incubated with anti-$p16^{ink4}$.

2.5. Colony formation

Six hundred tumor cells were seeded in triplicate in 6-well culture plates accordingly to previously published [15]. Trypsinization and suspension of single cells were carried out according to plating efficiencies.

2.6. Immunoblotting

Cells were seeded in 10 cm^3 dishes and treated as previously described. Protein lysates were loaded into 12% SDS–PAGE following electrophoresis and transferred to a polyvinyl difluoride membrane and incubated with anti-p53, anti-Acetyl-p53 (Lys382), anti-p21, and anti-GAPDH. The reaction was visualized using ECL SuperSignal West Pico Substrate.

2.7. Flow cytometry

Tumor cells were stained by propidium iodide to evaluate cell cycle distribution and stained for anti-BRD4 and anti-p-SIRT-1 antibodies following by secondary antibody conjugated with Alexa Fluor 488. Stem cell-like cancer cells were identified by high expression levels of aldehyde dehydrogenase and CD44-APC.

2.8. Apoptosis assay

Tumor cells receiving JQ1 were processed for cell viability using a Cell Vitality Assay Kit for Caspase-3/-7 (apoptotic cells) and Sytox (necrotic cells).

2.9. Senescence-associated beta-galactosidase staining

Senescent tumor cells were identified by SA-βGal using the SPiDER-βGal fluorescence kit from Dojindo Laboratories following the manufacturer's instructions.

2.10. Tumor sphere Formation assay

HNSCC cells were seeded on ultra-low attachment 6-well plates and cultured for seven days. Total number of spheres were counted and classified as holospheres, merospheres, or paraspheres based on size and borderline, as previously reported [16,17].

2.11. Tumor xenograft assay

Tumor cells were injected at a concentration of 5×10^6 cells into the flank of female nude mice. Within 3–4 weeks, xenograft tumors achieved a volume of 100 mm^3. JQ1 was administered intraperitoneally (50 mg/kg) once a day. Tumor growth was calculated according to previously reported [18]. The animal procedures were approved by the Institutional Animal Care and Use Committee (IACUC) at the University of Michigan and comply with the National Institutes of Health guide for the care and use of Laboratory Animals.

2.12. Statistical analysis

Statistical analysis was performed using GraphPad Prism (GraphPad Software, San Diego, CA). Statistical analysis was performed using unpaired Student's t-test or one-way ANOVA with a Bonferroni post hoc test. Asterisks denote statistical significance (*$p < 0.05$; **$p < 0.01$; ***$p < 0.001$; and NS $p > 0.05$).

See Supplemental Data for additional procedures.

3. Results

3.1. JQ1 efficiently reduces the levels of BRD4 and acetylated histone H4 in HNSSC

BRD4 is a member of the BET family of bromodomains that is associated with acetylated chromatin and found upregulated in solid tumors (http://www.cbioportal.org/). JQ1 is a small molecule that binds to the amino-terminal twin bromodomains of BRD4 acting as an important regulator of oncogenes by disrupting BRD4-driven oncogene enhancers [19]. Therefore, targeted inhibition of BRD4 may constitute a promising therapeutic strategy to target solid tumors.

In order to emphasize the potential use of JQ1 in HNSCC, we decide to access the expression levels of BRD4 in HNSCC using a tissue array comprised of nineteen different head and neck tumors and control normal oral mucosa (NOM). Interestingly we observed that NOM does not express high levels of BRD4 in epithelial cells, while all HNSCC samples expressed high levels of BRD4 (Fig. 1A and B) similar to previous findings [20]. Although HNSCC present high levels of BRD4

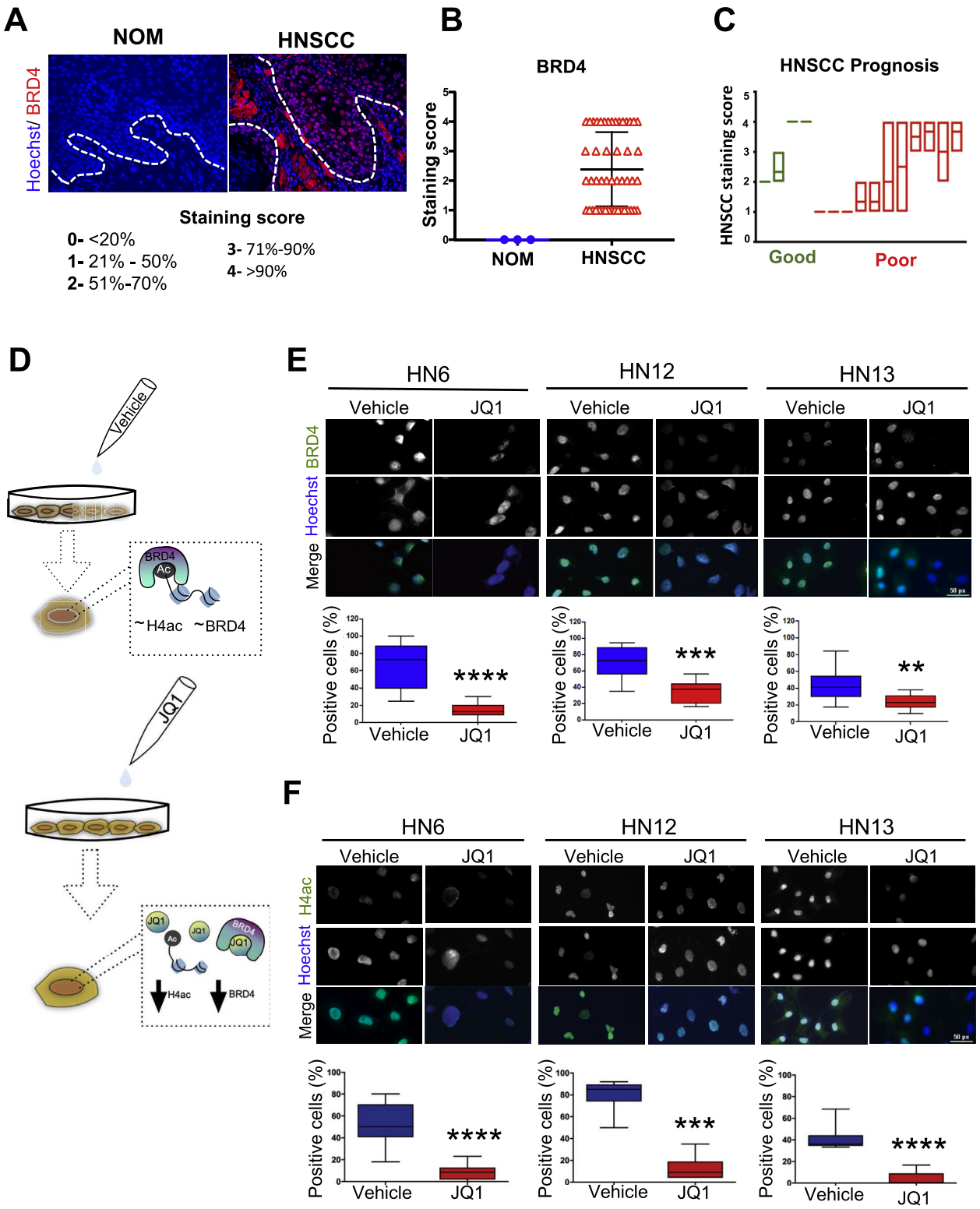

Fig. 1. HNSCC express high levels of BRD4. (A and B) HNSCC human samples (n = 19) express high levels of BRD4 compared with normal oral mucosa (NOM) (n = 3) tissue samples determined by immunofluorescence staining. (C) Total number of HNSCC tumor samples stratified accordingly with the clinical prognosis score. (D) Schematic representation of JQ1 administration to HNSCC. (E) Administration of JQ1 (1 μM) to HNSCC demonstrate reduced levels of BRD4 in all cell lines. (F) Identification of histone H4 (Lys 5,8,12, 16) levels in HNSCC receiving JQ1 and vehicle. Note the strong reduction of histone H4 (Lys 5,8,12, 16) levels. Data are represented as mean ± SD. Asterisk denotes significant differences (**p < 0.01; ***p < 0.001; ****p < 0.0001) two-tailed Student's t-test in (E), and (F).

expression, we did not observe a statistical difference among patients with good or poor prognosis as judged by clinical survival data, TNM classification, and treatment data from patients (Table 1) (Fig. 1C, ns p > 0.05). Next, we decided to explore if the administration of JQ1 could modify the protein levels of BRD4 and acetylated histone H4 (Lys 5, 8,12, and 16) (Fig. 1D). Tumor cells were exposed to JQ1 (1 μM) for 24hrs and BRD4 was used as a readout. We observed that JQ1 efficiently reduces BRD4 levels from HNSCC cells as judged by

Table 1
Patient survival, TNM staging, and therapy modality of HNSCC samples.

Case	Overall survival (5 years)	Prognosis	Tumor size	Regional Lymph Nodes	Distant Metastasis	Treatment
1	Alive	Good	T4	N2	M0	Surgery + Radiotherapy
2	Alive	Good	T4	N0	M1	Surgery + Radiotherapy
3	Alive	Good	T4	N1	M0	Surgery + Radiotherapy
4	Tumor related death	Bad	T4	N0	M0	Surgery + Chemotherapy
5	Alive	Not available	T4	N0	M0	Surgery + Radiotherapy
6	Dead by other reason	Bad	T2	N1	Mx	Surgery + Radiotherapy
7	Tumor related death	Bad	T4	N0	M0	Surgery
8	Alive	Bad	T1	N0	M0	Surgery
9	Alive	Bad	T2	N1	M0	Surgery + Radiotherapy
10	Alive	Bad	T4	N3	M0	Surgery + Radiotherapy
11	Alive	Bad	T2	N1	M0	Surgery + Radiotherapy
12	Alive	Good	T3	N0	M0	Surgery + Radiotherapy
13	Alive	Bad	T4	N2	M0	Surgery + Radiotherapy + Chemotherapy
14	Alive	Not available	T4	N2	M0	Surgery + Radiotherapy
15	Tumor related death	Bad	T3	Nx	Mx	Surgery + Radiotherapy
16	Alive	Bad	T3	N0	Mx	Surgery + Radiotherapy
17	Alive	Bad	T1	N1	M0	Surgery + Radiotherapy
18	Tumor related death	Not available	T2	N2C	M0	Surgery + Radiotherapy + Chemotherapy
19	Not available	Not available	Not available	Not available	Not available	Not available

immunofluorescence (Fig. 1E) and flow cytometry (Suppl. Fig. 1B) (*p < 0.05, **p < 0.01, ****p < 0.0001) as previously reported [21,22]. Similar to BDR4, we also observed that JQ1 efficiently reduced the levels of acetylated histone H4 from all analyzed HNSCC cells (Fig. 1F) (***p < 0.01, ****p < 0.0001). These findings are associated with the dual role of the chromatin reader BRD4 to regulate gene transcription and to modulate the chromatin landscape through the interaction with the histone acetyltransferase P300 [23]. Disruption of BRD4-histone interaction is known to selective deacetylation of histones H3 and H4 [24,25].

Although our results indicate that JQ1 is an effective inhibitor of BRD4-Histone H4 interaction in HNSCC tumors, we do not know if the displacement of BRD4-histone H4 binding has any effects on the biology of HNSCC.

3.2. JQ1 disrupts tumor ability to form colonies and induces cell cycle arrest

Following our initial findings on the ability of JQ1 to disrupt BRD4-histone H4 binding, we decided to explore the effects of bromodomain inhibitors on tumor growth. Using a clonogenic assay, we observed that JQ1 was able to disrupt the colony forming capability of HNSCC cells (Fig. 2A, ***p < 0.001, ****p < 0.0001). Microscopic analysis of tumor cells exposed to JQ1 revealed the presence of viable cells (Fig. 2B). These results are suggestive of cells growth arrest and the potential activation of cellular quiescence. Using flow cytometry, we decided to explore the effects of JQ1 on the cell cycle of all HNSCC cells. We observed that administration of JQ1 resulted in a G0/G1 cell cycle arrest in all 3 HNSCC cell lines and reduced G2 and S phases (Fig. 2C and D). Combined, this data strongly suggests a transition of tumor cells from a proliferative stage characterized by the presence of G2/M and S phases (Fig. 2D_vehicle) to a quiescent phase were the majority of tumor cells are found in G0/G1 (Fig. 2D_JQ1). Of note, HN13 was the only cell line showing high basal levels of apoptotic as detected by Propidium Iodine (Fig. 2C and D). To better characterize the JQ1-associated apoptosis phenotype observed during cell cycle analysis, we sought to use a more sensitive assay to determine the apoptosis levels in all tumor cell lines. We found that the effects of JQ1 are, at least in part, associated with the activation of apoptosis in HN6 and HN12 cell lines as judged by the accumulation of caspase 3 and caspase 7 using flow cytometry (Fig. 3A and B, *p < 0.05, ****p < 0.0001). Interestingly, HN13 cells present high levels of apoptosis in the control group, similar to the levels observed during the administration of JQ1 (Fig. 3A and B, ns p > 0.05).

3.3. JQ1 induces cellular senescence and downregulation of SIRT1

Following our unexpected findings on JQ1-induced G0/G1 cell cycle arrest, we observed that JQ1 also induces tumor cells to undergo senescence within 72 h of treatment (Fig. 4A and B (baseline-corrected), and Suppl. Fig. 3B (total protein expression levels)). Cellular senescence can be identified by the accumulation of $p16^{ink4}$, an essential mechanism epigenetically controlled by the Polycomb group of proteins (PcG) [26]. Interestingly, all tumor cell lines presented a baseline expression of $p16^{ink4}$ that was intensified upon administration of JQ1 (Fig. 4B) (**p < 0.01). We have also detected the increased accumulation of senescence-associated beta-galactosidase (SA-β-Gal) in tumor cells exposed to JQ1. SA-β-Gal is a well-known marker for cellular senescence (Fig. 4C and Suppl. Fig. 3A (****p < 0.0001).

In normal and neoplastic cells, the NAD^+-dependent Class III histone deacetylase SIRT1 has been shown to antagonize cellular senescence. Here we show that JQ1-drive disruption of BRD4/histone interaction reduced the expression levels of phospho-$SIRT1^{ser47}$ in all tumor cell lines as determined by immunofluorescence (Fig. 4D; *p < 0.05; **p < 0.01; ****p < 0.0001), and by flow cytometry (Suppl. Fig. 1C; *p < 0.05; **p < 0.01). Surprisingly, administration of JQ1 also reduces total levels of acetyl p53 (active) [27] in HN6 and HN13 cells, whereas HN12 have a point mutation in exon seven splice donor motif and does not express p53 [28]. While phosphorylation of SIRT1 typically leads to the accumulation of p53, JQ1-driven dephosphorylation of SIRT1 also reduced total protein levels of p53 (Fig. 4E and Suppl. Fig. 1A). It is interesting to note that HN6 and HN13 also present mutations on TP53 (missense), and that point and missense mutations observed in our cell lines have been shown to induce a dominant negative effect over wild-type p53 as previously described [28].

Next, we decided further explore the data on JQ1-induced cell cycle arrest of tumor cells by analyzing the expression levels of p21, a molecule known to induce G0 arrest and cellular quiescence when present in high levels [29]. Using lysates from tumor cells treated with JQ1 at 1 μM and 10 μM we observed that p21 is absent from vehicle-treated cells but starts to accumulate at low doses of JQ1 (1 μM) (Fig. 4E). It is also interesting to note that failure of mutant p53 proteins to transactivate p21 is often associated with uncontrolled proliferation [30], however, in our study, JQ1-induced activation of p21 and the accumulation of senescent cells suggests a p53-independent pathway.

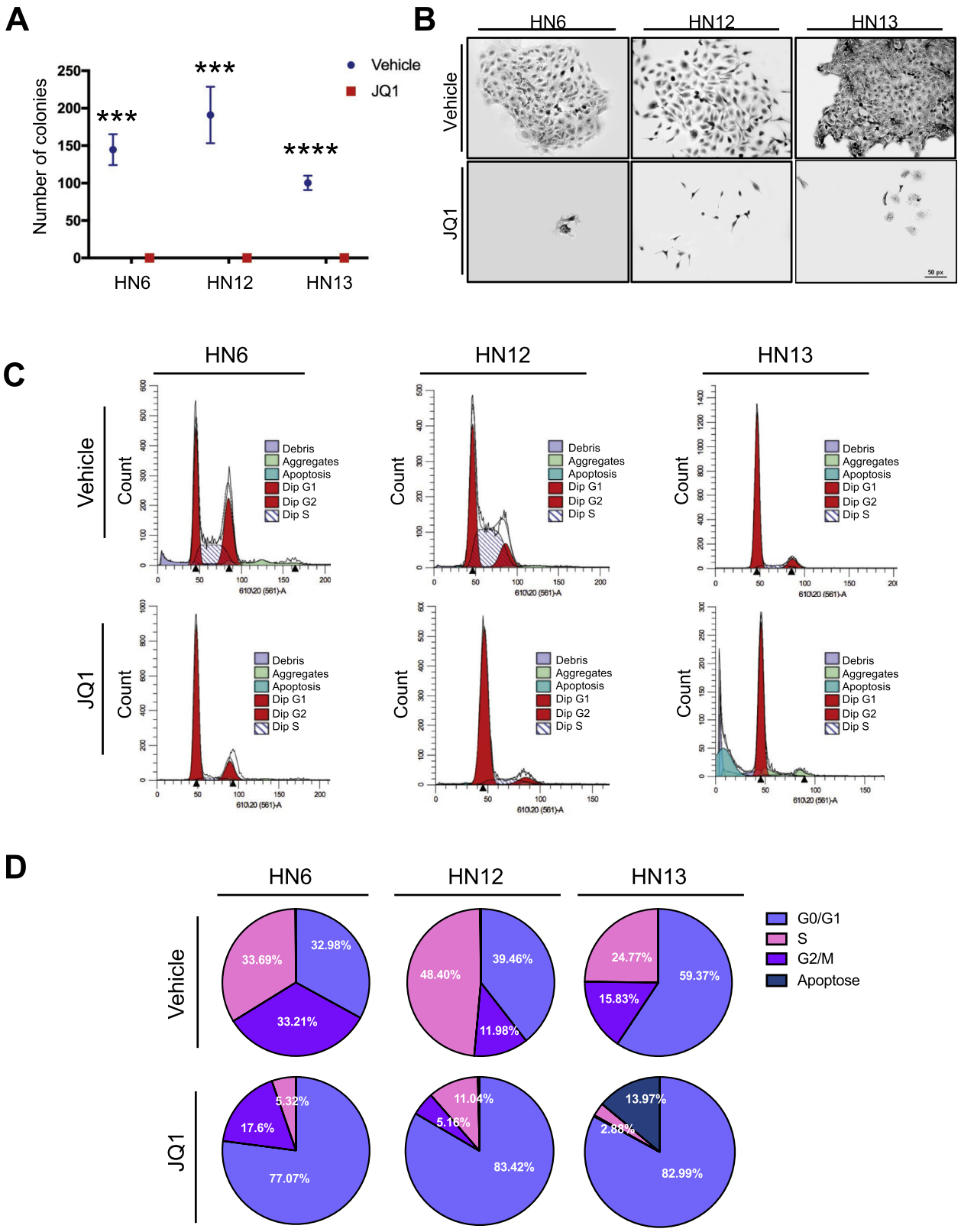

Fig. 2. JQ1 prevents colony formation and induces cell cycle arrest. (A) Graphic of total number of colonies from HN6, HN12, and HN13 cells lines receiving JQ1 or vehicle for 7days (1 μM - 600 cell seeded per well). Note the ability of JQ1 to prevent colony formation in all analyzed cell lines. (B) Representative images of colonies from all 3 cell lines receiving JQ1 and vehicle. Note that cells receiving JQ1 do not form colonies as defined by more than 50 cells. (C) Flow cytometry of tumor cells receiving vehicle and JQ1 for 24 h and stained with propidium iodide to evaluate cell cycle. (D) Pie graphic representing changes on cell cycle phases in all HNSCC cells upon administration of JQ1. Note that JQ1 treatment increases the number of tumor cells undergoing cycle arrest in G0/G1 phase. . Data are represented as mean ± SD. Asterisk denotes significant differences (***$p < 0.001$; ****$p < 0.0001$) one-way ANOVA with a Bonferroni post hoc test in (A).

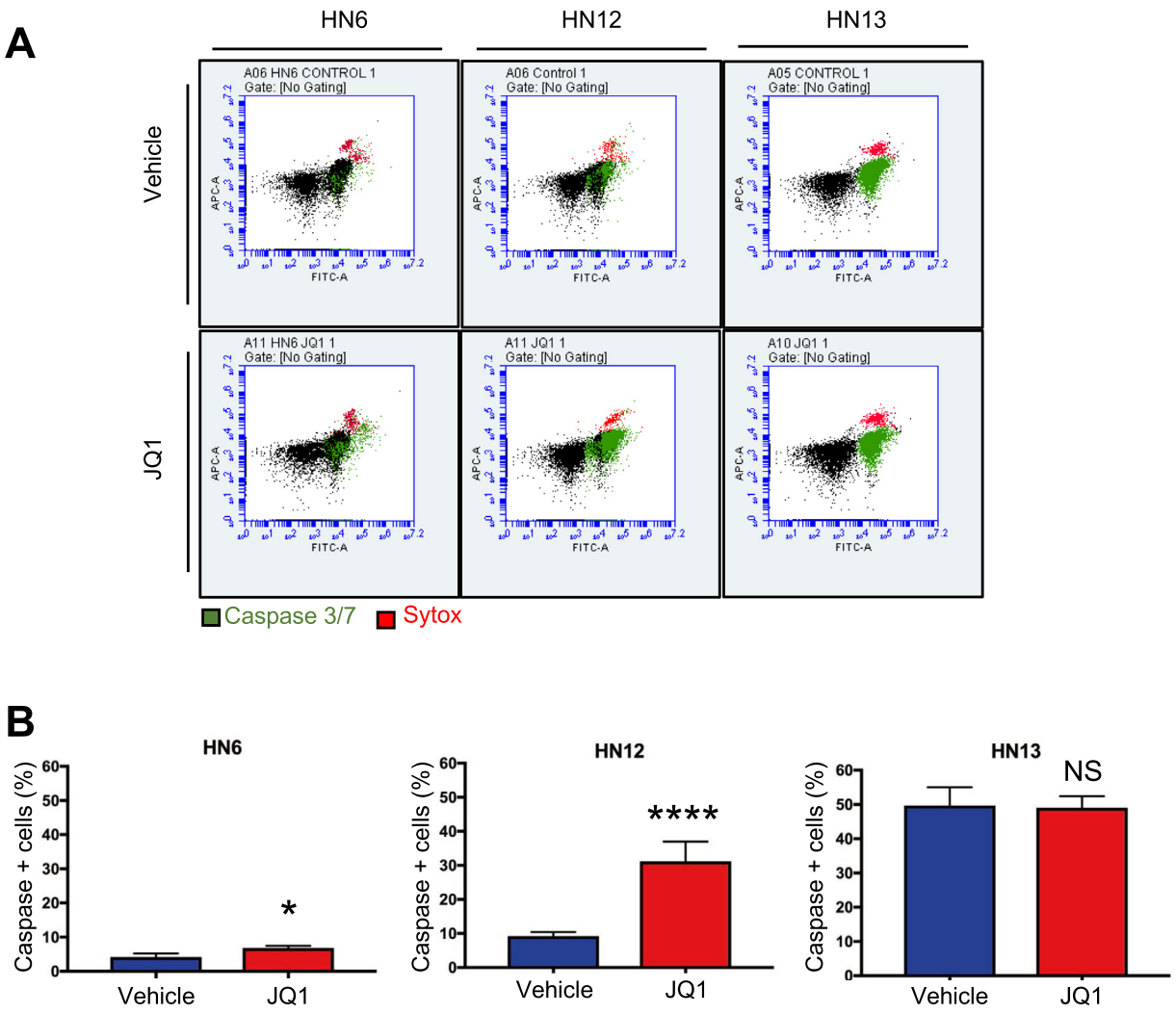

Fig. 3. JQ1 induces apoptosis in HNSCC cells. (A and B) Representative images of flow cytometry of HNSCC cells receiving JQ1 and vehicle show caspase 3/7 positive cells (apoptotic cells) represented in green and Sytox positive cells (necrotic cells) represented in Red. Note that JQ1 administration resulted in increased apoptosis in two out of the three analyzed tumor cell lines. HN13 cell line presents high levels (~50%) of caspase 3/7 positive cells in the control group. Data are represented as mean ± SD. Asterisk denotes significant differences (*p < 0.05; ****p < 0.0001, ns p > 0.05), two-tailed Student's t-test in (A) and (B). (For interpretation of the references to colour in this figure legend, the reader is referred to the Web version of this article.)

3.4. JQ1 reduces the population of stem cells-like cancer cells and halts tumor growth

We have previously shown that HDAC inhibitors such as Vorinostat, and TSA are capable of disrupting tumor spheres and reducing the population of $ALDH^{Bright}$ $CD44^{+}$ cells in vitro and in vivo [4,6,7]. Tumor cells presenting high levels of aldehyde dehydrogenases (ALDH) enzymatic activity ($ALDH^{Bright}$) and $CD44^{+}$ cells are sought to contain stem cell properties [31,32].

Here we explored if the displacement of BRD4-Histone H4 binding would impact the population of stem cells-like cancer cells. We observed that administration of JQ1 reduced the number of $ALDH^{Bright}$/$CD44^{+}$ cancer cells from two of our tumor cell lines (Fig. 5A and B, *p < 0.05, **p < 0.01.). We further performed a tumorsphere assay for our HNSCC cell lines. Our data demonstrate that different cell lines respond slightly different to JQ1. However, the sphere-forming potential of all cell lines was impacted by JQ1 (Suppl Fig. 2A and 2B). HN13 cell line did not show a reduction in the total number of spheres upon JQ1 administration similar to the observed using ALDH and CD44 markers, however, when carefully subcategorizing tumor spheres in holoclones, meroclones, and paraclones, we observed that JQ1 was particularly effective over holoclones compared to mero and paraclones from HN13 cells (Suppl. Fig. 2C). JQ1 was also effective in reducing the overall number of tumorspheres from HN6 and HN12 cell lines.

Following our promising results, we decided to evaluate if in vivo administration of JQ1 would impact tumor growth. Xenografts were generated using HNSCC cells (HN12) injected in the flanks of Foxn1(nu) (Jackson Laboratory, Bar Harbor, Maine) mice (n = 6 mice/group). After tumors achieved 100 mm^3, mice received IP injections of JQ1 (50 mg/kg per day) for 30 days. Control mice received vehicle alone (DMSO diluted in 1× PBS + 5% Tween 80). After 30 days of JQ1 administration, we observed a significant reduction in tumor growth compared to the vehicle group (Fig. 5C and D *p < 0.05, **p < 0.01). Based on our previous findings on JQ1-induced cell cycle arrest and activation of cellular senescence, we speculate that the reduced tumor mass observed in our xenograft tumors could be associated with the activation of cellular senescence. Indeed, we found that tumors receiving JQ1 had a higher number of senescent cells (Fig. 5C_ $p16^{ink4}$ and 5E, **p < 0.01). Along $p16^{ink4}$, the accumulation of γ-$H2AX^{ser129}$ is associated with telomere shortening of aging cells and organisms, and with the activation of cellular senescence through different mechanisms, including oncogene-induced-senescence (OIS) [33–36]. Here we show that administration of JQ1 also resulted in the accumulation of γ-$H2AX^{ser129}$ along $p16^{ink4}$ in tumor cells (Fig. 5F) (*p < 0.05). Similar

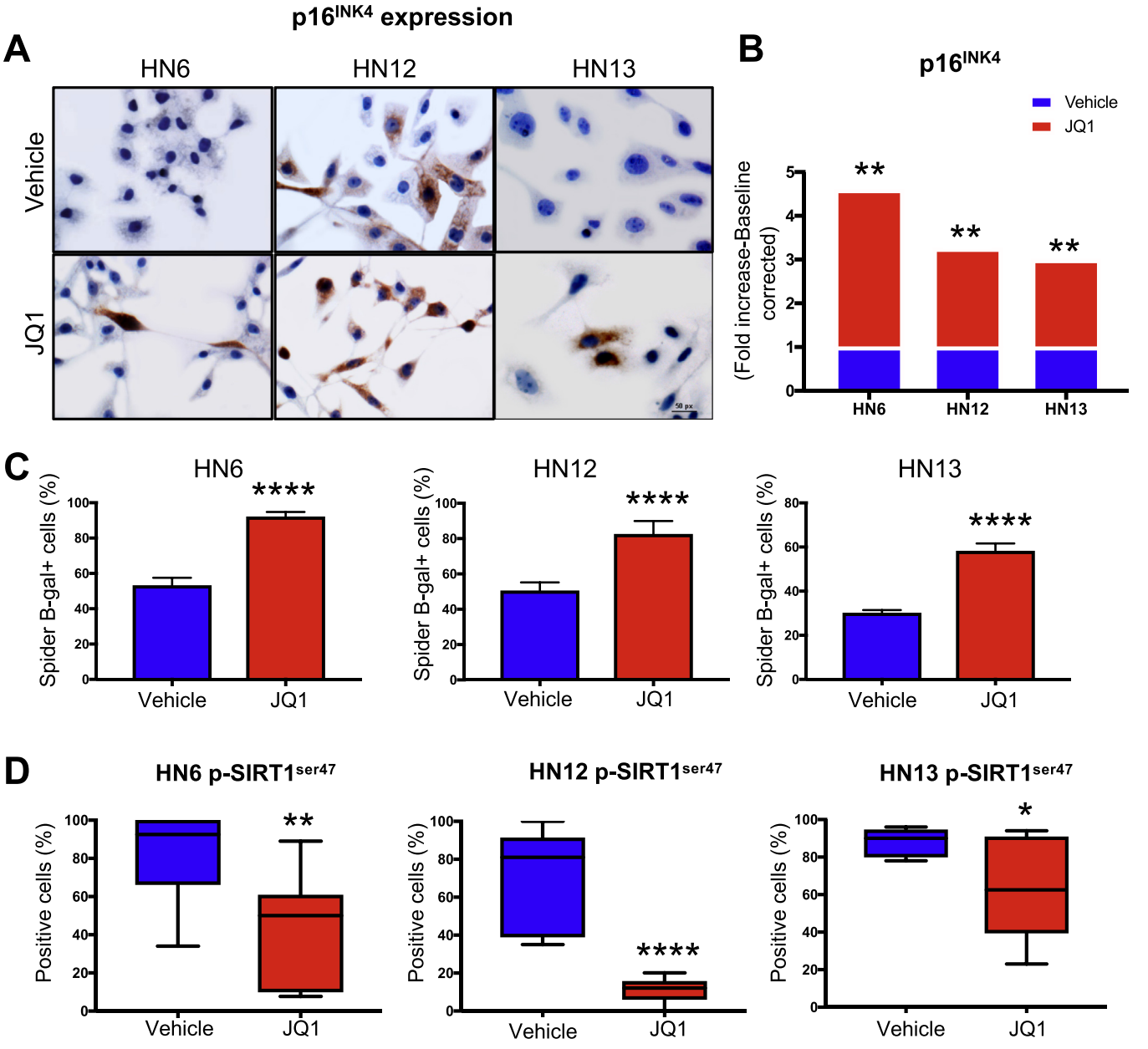

(caption on next page)

Fig. 4. JQ1 reduces levels of p53 expression or activates cellular senescence. (A) Representative images of $p16^{ink4}$ immunostaining of tumor cell lines (400× magnification). Immunohistochemistry assay shows JQ1 increases $p16^{ink4}$ expression in HN6, HN12, and HN13 cell lines. (B) Column representation of fold increase of $p16^{ink4}$ expression (baseline corrected) upon administration of JQ1 or vehicle. Note an HN6, HN12, HN13 fold increase of 3.6, 2.26 and 2 respectively over baseline (vehicle) (**$p < 0.01$, two-tailed Student's t-test). (C) Senescence-associated beta-galactosidase (SA-β-gal) assay detected senescent cancer cells in HN6, HN12, and HN13 upon administration of JQ1 (****$p < 0.0001$). (D) Immunofluorescence labeling of p-$Sirt1^{ser47}$ expression in tumor cells receiving JQ1 or vehicle for 24 h. Asterisk denotes significant differences (*$p < 0.05$; **$p < 0.01$; ****$p < 0.0001$, data are represented as mean ± SD, two-tailed Student's t-test). (E) Western blot analysis of p53, acetyl-p53 (lys382), p21, and GAPDH expression levels upon administration of JQ1 at 1 μM, and 10 μM concentration or vehicle.

to our in vitro data, xenografts receiving JQ1 also presented a statistically significant reduction on the levels of phospho-$SIRT1^{ser47}$ (Fig. 5G, ***$p < 0.001$). Following, we decided to access the presence of stem cells-like cancer cells within the xenograft tumors receiving JQ1. We found that JQ1 significantly reduced the number of ALDH1A1 positive cells (Fig. 5H, *$p < 0.05$).

Overall, our data show that interfering with the BRD4/histone H4 binding using JQ1 is relevant to HNSCC biology as it disrupts colony formation, induces cell cycle arrest, reduces the population of $ALDH^{Bright}/CD44^{+}$ cells, and activates cellular senescence in vitro and in vivo (Fig. 6).

4. Discussion

The epigenome constitutes a powerful molecular modulator of our genome responsible for the constant adaptation of our body to environmental changes. However, during carcinogenesis, the epigenome is also modified and to a certain extent, reprogramed, thereby facilitating cancer initiation and progression.

Perhaps one of the most notorious deregulated tumor suppressor genes in cancer history is the TP53. Acetylation of p53 at lysine k382 resulting in prolonged protein half-life due to reducing ubiquitination [37]. Here we used tumor cells containing common p53 point and missense mutations and presenting a dominant negative effect over wild-type p53 protein [28,38].

Interestingly, we observed that interfering with BRD4/histone H4 interaction resulted in the deacetylation of p53. To our knowledge, this is the first time that JQ1 is shown to downregulate acetylated p53 (Lys382) in head and neck tumors. Total protein levels of p53 were also downregulated by JQ1 suggesting that JQ1 may be effective in reducing the levels of p53. Similar results have been demonstrated in other tumors, including medulloblastoma cell lines that show downregulation of the TP53 pathway along with downregulation of E2F, MYC, and cell cycle pathways [39]. B-precursor acute lymphoblastic leukemia cell lines also respond to JQ1 by reducing the expression of phosphorylated p53 (ser15) [40]. Administration of JQ1 induces the activation of cellular senescence in medulloblastoma cell lines, in B-precursor acute lymphoblastic leukemia cell lines, and Chondrosarcoma cells [41]. Of interest to our study, p21 was also observed upregulated in Chondrosarcoma cells undergoing senescence in a p53 independent way. Yet, the molecular signaling involving JQ1-induced downregulation of p53 remain unknown.

In search for a mechanism involved in the JQ1-induced activation of cancer senescence, we looked into the expression levels of SIRT1, a class II histone deacetylases NAD + dependent associated with gene expression, cell cycle regulation, apoptosis, DNA repair, metabolism and lifespan [42,43]. Indeed, downregulation of SIRT1 is found in aging organisms and during the activation of cellular senescence [44]. Furthermore, SIRT1 is found downregulated in endothelial progenitor cells from the umbilical cord that are undergoing cellular senescence. It is also known that some pharmacological agents like Resveratrol are capable of inducing downregulation of SIRT1, leading to the activation of cellular senescence in fibroblasts [45,46]. In our study, we can only demonstrate a correlation of SIRT1 expression and the accumulation of cellular senescence, and we cannot discard additional pathways that may be involved in the activation of cancer senescence. Physiological conditions such as the accumulation of reactive oxygen species (ROS) also inhibits SIRT1 leading to the acetylation of p53 and premature senescence of MEFs [47]. Indeed, there is a lot to be explored on the mechanism of JQ1-driven downregulation of SIRT1 and acetyl p53, and further the reactivation of p21 upon downregulation of acetyl p53. Aligned with these observations, Elbendary et al. suggested that p21 may also be regulated by a p53-independent pathway [30].

HNSCC are heterogeneous tumors presenting a complex genomic landscape [48–50]. Predisposition factors like HPV infection and tobacco use are often associated with tumors containing high copy number alterations (CNA). A subset of oral tumors, however, are characterized by the presence of low CNA and therefore driven by mutations ("M" class). Such differences in the HNSCC tumor landscape demonstrates the need for patient stratification and the identification of personalized therapies targeting specific molecular signatures. This is true for the JQ1-induced cellular senescence. Activation of cellular senescence requires wildtype CDKN2A gene expression that encodes $p16^{ink4}$. It is important to note that we used HNSCC cell lines presenting wildtype CDKN2A gene [51] that represents around 50% of all HNSCC (TCGA database). The other half of HNSCC cases are characterized by the presence of mutations on CDKN2A gene (19%), deep deletions (30%), and a combination of fusion and various other alterations in less than 1% of all cases from the TCGA database.

Cellular senescence is a normal process characterized by an irreversible cell cycle arrest. However, cancer cells skip this scenario and divide infinitely. Avoidance of cellular senescence is achieved by the telomerase activation in cancers, DNA damage, and inactivation of tumor suppressors [52]. Small molecules capable of modulating the epigenome like HDAC and bromodomain inhibitors have shown a common trend in activating cellular senescence in normal and malignant tissues, including head and neck cancers [6,53,54] [55,56].

Along with the activation of cellular senescence, we have also shown that HDAC inhibitors deregulate stem cell-associated genes resulting in disruption of cancer stem cells [4,6,7,57,58]. The process of cellular senescence is convoluted and not completely understood. For instance, in B-cells lymphomas, switchable models of senescence targeting H3K9me3 or p53 triggered cell scape from senescence and reactivation of the cell cycle and Wnt-dependent clonogenic potential [59]. Tumor plasticity, therefore, seems strongly associated with the modification of histones and potentially regulated by changes in the bromodomain levels and activity.

Overall the effect of gene mutations on the epigenome machinery remains unknown; however, gradually it is becoming clear that epigenetic modifications play a key role in the control of tumor suppressor genes like we have demonstrated with the reactivation of p21, and consequently tumor senescence.

Author contributions

R.M.C. and C.H.S. conceived the idea and guided experiments. L.P.W. performed the experiments. V.Q.Y helped to perform the experiments. M.D.M, P.A.V., C.H.S., and R.M.C. analyzed and interpreted the results. L.P.W., M.D.M., and R.M.C. wrote the manuscript with inputs from all authors. All authors discussed the results and gave final approval of the manuscript.

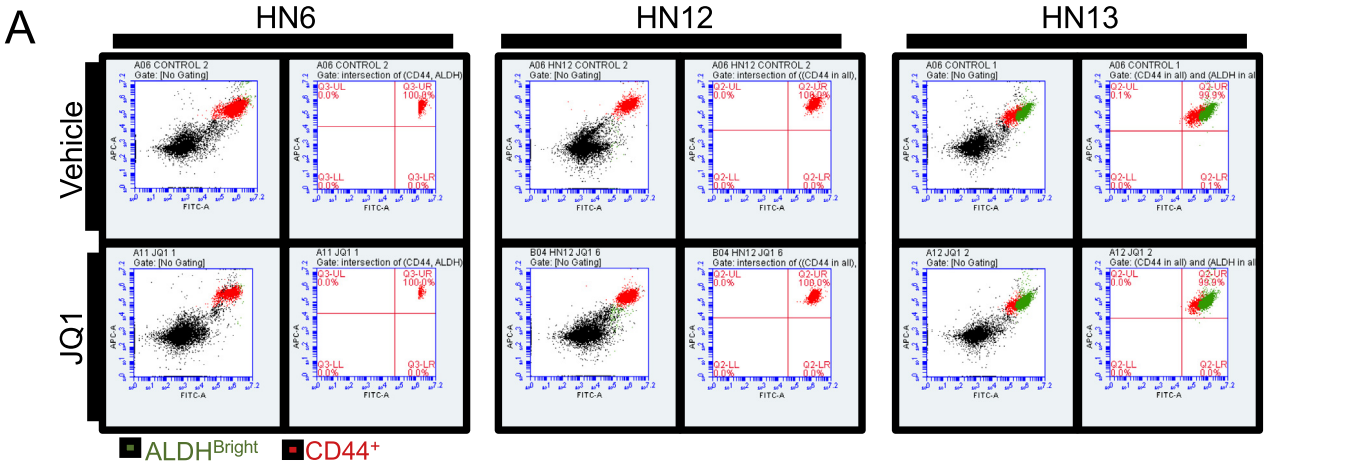

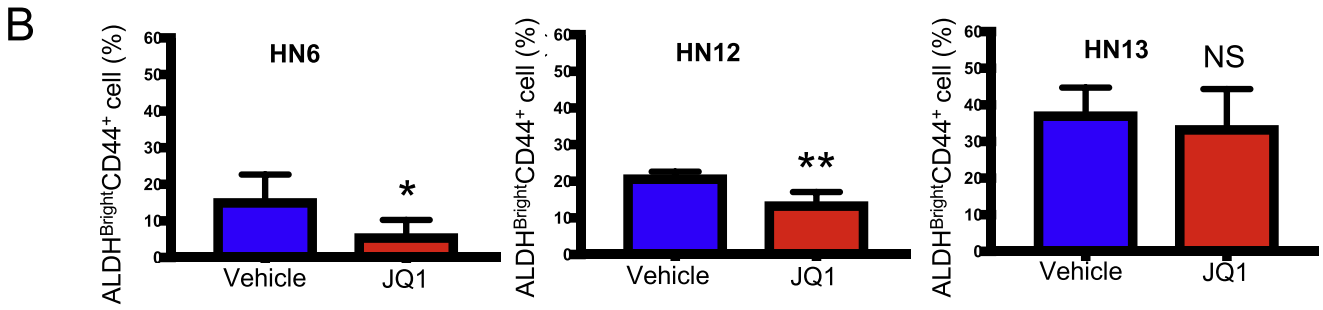

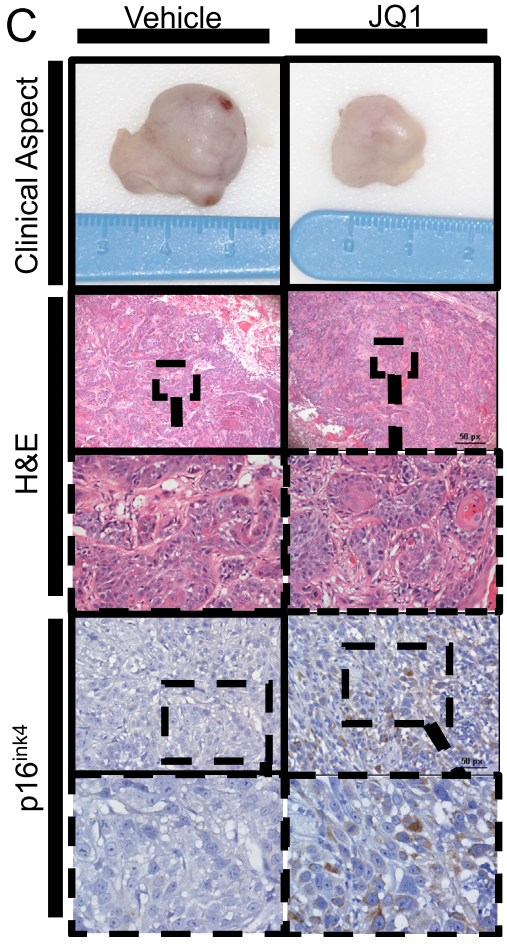

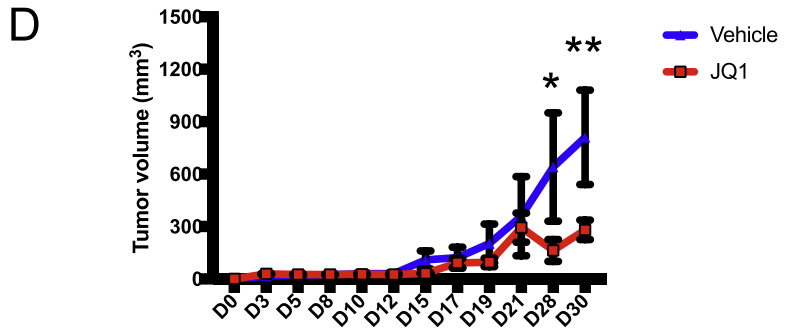

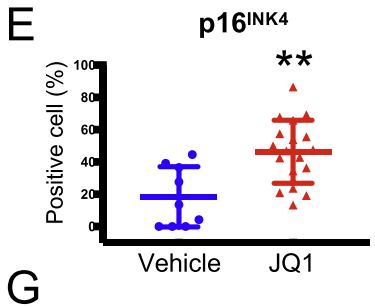

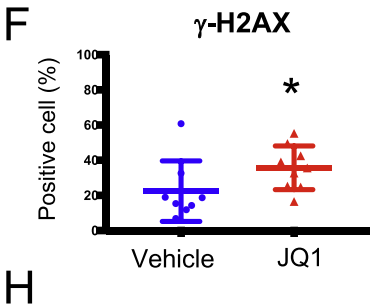

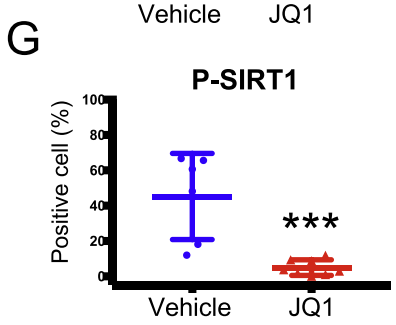

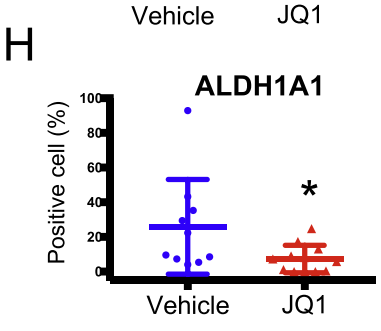

(caption on next page)

Fig. 5. JQ1 target cancer stem cells in vitro and in vivo. (A) Representative images of $ALDH^{Bright}$ (green) and $CD44^{+}$ (red) populations analyzed by flow cytometry. (B) Graphical representation of the total number of $ALDH^{Bright}/CD44^{+}$ bright cells identified in all three analyzed tumor cell lines. JQ1 group reduces cancer stem cell-like in two (HN6 and HN12) of three cell lines. Asterisk denotes significant differences (ns $p > 0.05$, *$p < 0.05$; **$p < 0.01$). (C) Representative images of tumor xenografts growing in nu/nu mice receiving JQ1 or vehicle. Histological appearance of tumor xenografts demonstrates similar histological appearance between JQ1 and vehicle groups. Immunohistochemistry staining for $p16^{ink4}$ depicts an increasing number of positive tumor cells upon administration of JQ1. (D) Graphical representation of tumor growth from mice receiving vehicle or JQ1. Note a reduced tumor volume on JQ1-treated mice starting at day 28 (*$p < 0.05$; **$p < 0.01$). (E) Quantification of positive cells for $p16^{ink4}$ in JQ1 and vehicle groups. Note increased expression of $p16^{ink4}$ in JQ1-treated tumors suggesting augmented cellular senescence (**$p < 0.01$). (F) Accumulation of DNA double-strand breaks in xenograft tumor samples receiving JQ1 as a marker for genomic instability (*$p < 0.05$). (G) Tumor xenografts present increased expression of $p\text{-}SIRT1^{ser47}$ as determined by immunostaining (***$p < 0.001$). (H) Graphical representation of the expression levels of ALDH1A1 positive cells present in xenograft tumors receiving JQ1 or vehicle (*$p < 0.05$). Data are represented as mean ± SD. Two-tailed Student's t-test in (B), (E), (F), (G), (H) and one-way ANOVA with a Bonferroni post hoc test in (D). (For interpretation of the references to colour in this figure legend, the reader is referred to the Web version of this article.)

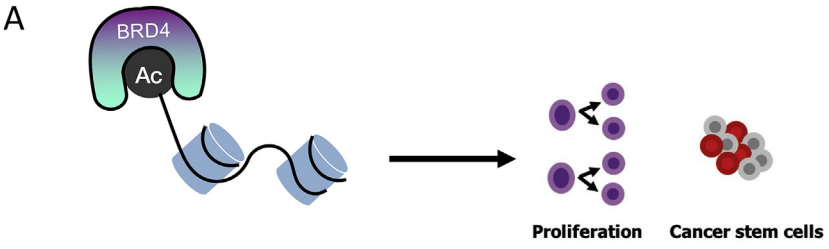

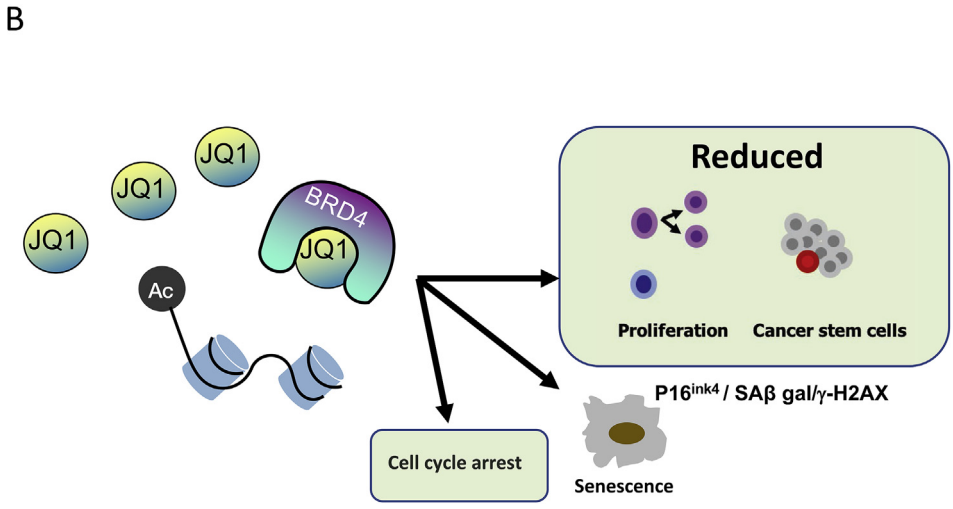

Fig. 6. Schematic illustration of JQ1 effect over HNSCC. (A) BRD4 as a reader of acetyl-lysine histone leading to tumor proliferation and the presence of stem cells-like cancer cells (red dots). (B) JQ1 displacement of histone from the BRD4 acetyl-lysine histone binding site resulting in reduced tumor proliferation, reduced number of stem cell-like cells (red dots), cell cycle arrest, and activation of cellular senescence. (For interpretation of the references to colour in this figure legend, the reader is referred to the Web version of this article.)

Declaration of interests

None declared.

Acknowledgments

This work was conducted during a visiting scholar period at the University of Michigan, and partially sponsored by the National Council for Scientific and Technological Development (CNPq) within the Brazilian Ministry of Science and Technology (grant n. 201959/2015-1), and by the University of Michigan Cancer Center Support Grant (P30 CA046592). This grant was funded by the University of Michigan School of Dentistry faculty grant, and by The Robert Wood Johnson Foundation – (AMFDP- 72425). The authors declare no potential conflicts of interest concerning the authorship and/or publication of this article.

Appendix A. Supplementary data

Supplementary data to this article can be found online at https://doi.org/10.1016/j.canlet.2019.06.019.

References

[1] S. Warnakulasuriya, Living with oral cancer: epidemiology with particular reference to prevalence and life-style changes that influence survival, Oral Oncol. 46 (2010) 407–410.
[2] L.P. Webber, V.P. Wagner, M. Curra, P.A. Vargas, L. Meurer, V.C. Carrard, C.H. Squarize, R.M. Castilho, M.D. Martins, Hypoacetylation of acetyl-histone H3 (H3K9ac) as marker of poor prognosis in oral cancer, Histopathology 71 (2017) 278–286.
[3] L.O. Almeida, A.C. Abrahao, L.K. Rosselli-Murai, F.S. Giudice, C. Zagni, A.M. Leopoldino, C.H. Squarize, R.M. Castilho, NFkappaB mediates cisplatin resistance through histone modifications in head and neck squamous cell carcinoma (HNSCC), FEBS Open Bio 4 (2014) 96–104.
[4] V.P. Wagner, M.D. Martins, M.A.T. Martins, L.O. Almeida, K.A. Warner, J.E. Nor, C.H. Squarize, R.M. Castilho, Targeting histone deacetylase and NFkappaB signaling as a novel therapy for Mucoepidermoid Carcinomas, Sci. Rep. 8 (2018) 2065.
[5] R.M. Castilho, C.H. Squarize, L.O. Almeida, Epigenetic modifications and head and neck cancer: implications for tumor progression and resistance to therapy, Int. J. Mol. Sci. 18 (2017).
[6] L.O. Almeida, D.M. Guimaraes, M.D. Martins, M.A.T. Martins, K.A. Warner, J.E. Nor, R.M. Castilho, C.H. Squarize, Unlocking the chromatin of adenoid cystic carcinomas using HDAC inhibitors sensitize cancer stem cells to cisplatin and induces tumor senescence, Stem Cell Res. 21 (2017) 94–105.
[7] D.M. Guimaraes, L.O. Almeida, M.D. Martins, K.A. Warner, A.R. Silva, P.A. Vargas, F.D. Nunes, C.H. Squarize, J.E. Nor, R.M. Castilho, Sensitizing mucoepidermoid carcinomas to chemotherapy by targeted disruption of cancer stem cells, Oncotarget 7 (2016) 42447–42460.
[8] R. Di Micco, B. Fontanals-Cirera, V. Low, P. Ntziachristos, S.K. Yuen, C.D. Lovell,

I. Dolgalev, Y. Yonekubo, G. Zhang, E. Rusinova, G. Gerona-Navarro, M. Canamero, M. Ohlmeyer, I. Aifantis, M.M. Zhou, A. Tsirigos, E. Hernando, Control of embryonic stem cell identity by BRD4-dependent transcriptional elongation of super-enhancer-associated pluripotency genes, Cell Rep. 9 (2014) 234–247.
[9] W. Liu, P. Stein, X. Cheng, W. Yang, N.Y. Shao, E.E. Morrisey, R.M. Schultz, J. You, BRD4 regulates Nanog expression in mouse embryonic stem cells and pre-implantation embryos, Cell Death Differ. 21 (2014) 1950–1960.
[10] G.A. Horne, H.J. Stewart, J. Dickson, S. Knapp, B. Ramsahoye, T. Chevassut, Nanog requires BRD4 to maintain murine embryonic stem cell pluripotency and is suppressed by bromodomain inhibitor JQ1 together with Lefty1, Stem Cell. Dev. 24 (2015) 879–891.
[11] M. Gonzales-Cope, S. Sidoli, N.V. Bhanu, K.J. Won, B.A. Garcia, Histone H4 acetylation and the epigenetic reader Brd4 are critical regulators of pluripotency in embryonic stem cells, BMC Genomics 17 (2016) 95.
[12] P. Filippakopoulos, J. Qi, S. Picaud, Y. Shen, W.B. Smith, O. Fedorov, E.M. Morse, T. Keates, T.T. Hickman, I. Felletar, M. Philpott, S. Munro, M.R. McKeown, Y. Wang, A.L. Christie, N. West, M.J. Cameron, B. Schwartz, T.D. Heightman, N. La Thangue, C.A. French, O. Wiest, A.L. Kung, S. Knapp, J.E. Bradner, Selective inhibition of BET bromodomains, Nature 468 (2010) 1067–1073.
[13] J.E. Delmore, G.C. Issa, M.E. Lemieux, P.B. Rahl, J. Shi, H.M. Jacobs, E. Kastritis, T. Gilpatrick, R.M. Paranal, J. Qi, M. Chesi, A.C. Schinzel, M.R. McKeown, T.P. Heffernan, C.R. Vakoc, P.L. Bergsagel, I.M. Ghobrial, P.G. Richardson, R.A. Young, W.C. Hahn, K.C. Anderson, A.L. Kung, J.E. Bradner, C.S. Mitsiades, BET bromodomain inhibition as a therapeutic strategy to target c-Myc, Cell 146 (2011) 904–917.
[14] J. Jang, Y.J. Huh, H.J. Cho, B. Lee, J. Park, D.Y. Hwang, D.W. Kim, SIRT1 enhances the survival of human embryonic stem cells by promoting DNA repair, Stem Cell Reports 9 (2017) 629–641.
[15] N.A. Franken, H.M. Rodermond, J. Stap, J. Haveman, C. van Bree, Clonogenic assay of cells in vitro, Nat. Protoc. 1 (2006) 2315–2319.
[16] Y. Barrandon, H. Green, Three clonal types of keratinocyte with different capacities for multiplication, Proc. Natl. Acad. Sci. U. S. A. 84 (1987) 2302–2306.
[17] L.O. Almeida, D.M. Guimaraes, C.H. Squarize, R.M. Castilho, Profiling the behavior of distinct populations of head and neck cancer stem cells, Cancers (2016) 8.
[18] K. Enomoto, X. Zhu, S. Park, L. Zhao, Y.J. Zhu, M.C. Willingham, J. Qi, J.A. Copland, P. Meltzer, S.Y. Cheng, Targeting MYC as a therapeutic intervention for anaplastic thyroid cancer, J. Clin. Endocrinol. Metab. 102 (2017) 2268–2280.
[19] J. Loven, H.A. Hoke, C.Y. Lin, A. Lau, D.A. Orlando, C.R. Vakoc, J.E. Bradner, T.I. Lee, R.A. Young, Selective inhibition of tumor oncogenes by disruption of super-enhancers, Cell 153 (2013) 320–334.
[20] B. Leonard, T.M. Brand, R.A. O'Keefe, E.D. Lee, Y. Zeng, J.D. Kemmer, H. Li, J.R. Grandis, N.E. Bhola, BET inhibition overcomes receptor tyrosine kinase-mediated cetuximab resistance in HNSCC, Cancer Res. 78 (2018) 4331–4343.
[21] M. Qu, X. Zhang, X. Hu, M. Dong, X. Pan, J. Bian, Q. Zhou, BRD4 inhibitor JQ1 inhibits and reverses mechanical injury-induced corneal scarring, Cell Death Dis. 4 (2018) 5.
[22] L. Wang, X. Wu, R. Wang, C. Yang, Z. Li, C. Wang, F. Zhang, P. Yang, BRD4 inhibition suppresses cell growth, migration and invasion of salivary adenoid cystic carcinoma, Biol. Res. 50 (2017) 19.
[23] T. Wu, Y.F. Kamikawa, M.E. Donohoe, Brd4's bromodomains mediate histone H3 acetylation and chromatin remodeling in pluripotent cells through P300 and Brg1, Cell Rep. 25 (2018) 1756–1771.
[24] E. Nicodeme, K.L. Jeffrey, U. Schaefer, S. Beinke, S. Dewell, C.W. Chung, R. Chandwani, I. Marazzi, P. Wilson, H. Coste, J. White, J. Kirilovsky, C.M. Rice, J.M. Lora, R.K. Prinjha, K. Lee, A. Tarakhovsky, Suppression of inflammation by a synthetic histone mimic, Nature 468 (2010) 1119–1123.
[25] A. Nishiyama, A. Dey, J. Miyazaki, K. Ozato, Brd4 is required for recovery from antimicrotubule drug-induced mitotic arrest: preservation of acetylated chromatin, Mol. Biol. Cell 17 (2006) 814–823.
[26] E. Simboeck, J.D. Ribeiro, S. Teichmann, L. Di Croce, Epigenetics and senescence: learning from the INK4-ARF locus, Biochem. Pharmacol. 82 (2011) 1361–1370.
[27] K. Sakaguchi, J.E. Herrera, S. Saito, T. Miki, M. Bustin, A. Vassilev, C.W. Anderson, E. Appella, DNA damage activates p53 through a phosphorylation-acetylation cascade, Genes Dev. 12 (1998) 2831–2841.
[28] W.A. Yeudall, J. Jakus, J.F. Ensley, K.C. Robbins, Functional characterization of p53 molecules expressed in human squamous cell carcinomas of the head and neck, Mol. Carcinog. 18 (1997) 89–96.
[29] S.L. Spencer, S.D. Cappell, F.C. Tsai, K.W. Overton, C.L. Wang, T. Meyer, The proliferation-quiescence decision is controlled by a bifurcation in CDK2 activity at mitotic exit, Cell 155 (2013) 369–383.
[30] A.A. Elbendary, F.D. Cirisano, A.C. Evans Jr., P.L. Davis, J.D. Iglehart, J.R. Marks, A. Berchuck, Relationship between p21 expression and mutation of the p53 tumor suppressor gene in normal and malignant ovarian epithelial cells, Clin. Cancer Res. 2 (1996) 1571–1575.
[31] M.E. Prince, R. Sivanandan, A. Kaczorowski, G.T. Wolf, M.J. Kaplan, P. Dalerba, I.L. Weissman, M.F. Clarke, L.E. Ailles, Identification of a subpopulation of cells with cancer stem cell properties in head and neck squamous cell carcinoma, Proc. Natl. Acad. Sci. U. S. A. 104 (2007) 973–978.
[32] M.R. Clay, M. Tabor, J.H. Owen, T.E. Carey, C.R. Bradford, G.T. Wolf, M.S. Wicha, M.E. Prince, Single-marker identification of head and neck squamous cell carcinoma cancer stem cells with aldehyde dehydrogenase, Head Neck 32 (2010) 1195–1201.
[33] M.G. Hovest, N. Bruggenolte, K.S. Hosseini, T. Krieg, G. Herrmann, Senescence of human fibroblasts after psoralen photoactivation is mediated by ATR kinase and persistent DNA damage foci at telomeres, Mol. Biol. Cell 17 (2006) 1758–1767.
[34] O.A. Sedelnikova, I. Horikawa, D.B. Zimonjic, N.C. Popescu, W.M. Bonner, J.C. Barrett, Senescing human cells and ageing mice accumulate DNA lesions with unrepairable double-strand breaks, Nat. Cell Biol. 6 (2004) 168–170.
[35] R.M. Castilho, C.H. Squarize, L.A. Chodosh, B.O. Williams, J.S. Gutkind, mTOR mediates Wnt-induced epidermal stem cell exhaustion and aging, Cell Stem Cell 5 (2009) 279–289.
[36] H. Liu, M.M. Fergusson, R.M. Castilho, J. Liu, L. Cao, J. Chen, D. Malide, Rovira II, D. Schimel, C.J. Kuo, J.S. Gutkind, P.M. Hwang, T. Finkel, Augmented Wnt signaling in a mammalian model of accelerated aging, Science 317 (2007) 803–806.
[37] Y. Zhao, S. Lu, L. Wu, G. Chai, H. Wang, Y. Chen, J. Sun, Y. Yu, W. Zhou, Q. Zheng, M. Wu, G.A. Otterson, W.G. Zhu, Acetylation of p53 at lysine 373/382 by the histone deacetylase inhibitor depsipeptide induces expression of p21(Waf1/Cip1), Mol. Cell. Biol. 26 (2006) 2782–2790.
[38] G. Zhou, Z. Liu, J.N. Myers, TP53 mutations in head and neck squamous cell carcinoma and their impact on disease progression and treatment response, J. Cell. Biochem. 117 (2016) 2682–2692.
[39] A. Henssen, T. Thor, A. Odersky, L. Heukamp, N. El-Hindy, A. Beckers, F. Speleman, K. Althoff, S. Schafers, A. Schramm, U. Sure, G. Fleischhack, A. Eggert, J.H. Schulte, BET bromodomain protein inhibition is a therapeutic option for medulloblastoma, Oncotarget 4 (2013) 2080–2095.
[40] D. Da Costa, A. Agathanggelou, T. Perry, V. Weston, E. Petermann, A. Zlatanou, C. Oldreive, W. Wei, G. Stewart, J. Longman, E. Smith, P. Kearns, S. Knapp, T. Stankovic, BET inhibition as a single or combined therapeutic approach in primary paediatric B-precursor acute lymphoblastic leukaemia, Blood Canc. J. 3 (2013) e126.
[41] H.T. Zhang, T. Gui, Y. Sang, J. Yang, Y.H. Li, G.H. Liang, T. Li, Q.Y. He, Z.G. Zha, The BET bromodomain inhibitor JQ1 suppresses chondrosarcoma cell growth via regulation of YAP/p21/c-Myc signaling, J. Cell. Biochem. 118 (2017) 2182–2192.
[42] M.D. Martins, R.M. Castilho, Histones: controlling tumor signaling circuitry, J. Carcinog. Mutagen. 1 (2013) 1–12.
[43] C.L. Brooks, W. Gu, How does SIRT1 affect metabolism, senescence and cancer? Nat. Rev. Canc. 9 (2009) 123–128.
[44] T. Hayakawa, M. Iwai, S. Aoki, K. Takimoto, M. Maruyama, W. Maruyama, N. Motoyama, SIRT1 suppresses the senescence-associated secretory phenotype through epigenetic gene regulation, PLoS One 10 (2015) e0116480.
[45] P.F. Vassallo, S. Simoncini, I. Ligi, A.L. Chateau, R. Bachelier, S. Robert, J. Morere, S. Fernandez, B. Guillet, M. Marcelli, E. Tellier, A. Pascal, U. Simeoni, F. Anfosso, F. Magdinier, F. Dignat-George, F. Sabatier, Accelerated senescence of cord blood endothelial progenitor cells in premature neonates is driven by SIRT1 decreased expression, Blood 123 (2014) 2116–2126.
[46] M. Kilic Eren, A. Kilincli, O. Eren, Resveratrol induced premature senescence is associated with DNA damage mediated SIRT1 and SIRT2 down-regulation, PLoS One 10 (2015) e0124837.
[47] D. Volonte, H. Zou, J.N. Bartholomew, Z. Liu, P.A. Morel, F. Galbiati, Oxidative stress-induced inhibition of Sirt1 by caveolin-1 promotes p53-dependent premature senescence and stimulates the secretion of interleukin 6 (IL-6), J. Biol. Chem. 290 (2015) 4202–4214.
[48] N. Stransky, A.M. Egloff, A.D. Tward, A.D. Kostic, K. Cibulskis, A. Sivachenko, G.V. Kryukov, M.S. Lawrence, C. Sougnez, A. McKenna, E. Shefler, A.H. Ramos, P. Stojanov, S.L. Carter, D. Voet, M.L. Cortes, D. Auclair, M.F. Berger, G. Saksena, C. Guiducci, R.C. Onofrio, M. Parkin, M. Romkes, J.L. Weissfeld, R.R. Seethala, L. Wang, C. Rangel-Escareno, J.C. Fernandez-Lopez, A. Hidalgo-Miranda, J. Melendez-Zajgla, W. Winckler, K. Ardlie, S.B. Gabriel, M. Meyerson, E.S. Lander, G. Getz, T.R. Golub, L.A. Garraway, J.R. Grandis, The mutational landscape of head and neck squamous cell carcinoma, Science 333 (2011) 1157–1160.
[49] N. Agrawal, M.J. Frederick, C.R. Pickering, C. Bettegowda, K. Chang, R.J. Li, C. Fakhry, T.X. Xie, J. Zhang, J. Wang, N. Zhang, A.K. El-Naggar, S.A. Jasser, J.N. Weinstein, L. Trevino, J.A. Drummond, D.M. Muzny, Y. Wu, L.D. Wood, R.H. Hruban, W.H. Westra, W.M. Koch, J.A. Califano, R.A. Gibbs, D. Sidransky, B. Vogelstein, V.E. Velculescu, N. Papadopoulos, D.A. Wheeler, K.W. Kinzler, J.N. Myers, Exome sequencing of head and neck squamous cell carcinoma reveals inactivating mutations in NOTCH1, Science 333 (2011) 1154–1157.
[50] N. Cancer, Genome Atlas, Comprehensive genomic characterization of head and neck squamous cell carcinomas, Nature 517 (2015) 576–582.
[51] D. Martin, M.C. Abba, A.A. Molinolo, L. Vitale-Cross, Z. Wang, M. Zaida, N.C. Delic, Y. Samuels, J.G. Lyons, J.S. Gutkind, The head and neck cancer cell oncogenome: a platform for the development of precision molecular therapies, Oncotarget 5 (2014) 8906–8923.
[52] W.C. Hahn, M. Meyerson, Telomerase activation, cellular immortalization and cancer, Ann. Med. 33 (2001) 123–129.
[53] G. Di Bernardo, T. Squillaro, C. Dell'Aversana, M. Miceli, M. Cipollaro, A. Cascino, L. Altucci, U. Galderisi, Histone deacetylase inhibitors promote apoptosis and senescence in human mesenchymal stem cells, Stem Cell. Dev. 18 (2009) 573–581.
[54] J.E. Vargas, E.C. Filippi-Chiela, T. Suhre, F.C. Kipper, D. Bonatto, G. Lenz, Inhibition of HDAC increases the senescence induced by natural polyphenols in glioma cells, Biochem. Cell Biol. 92 (2014) 297–304.
[55] W.S. Xu, G. Perez, L. Ngo, C.Y. Gui, P.A. Marks, Induction of polyploidy by histone deacetylase inhibitor: a pathway for antitumor effects, Cancer Res. 65 (2005) 7832–7839.
[56] C.C. Hsu, W.C. Chang, T.I. Hsu, J.J. Liu, S.H. Yeh, J.Y. Wang, J.P. Liou, C.Y. Ko, K.Y. Chang, J.Y. Chuang, Suberoylanilide hydroxamic acid represses glioma stem-like cells, J. Biomed. Sci. 23 (2016) 81.
[57] M.H. Cai, X.G. Xu, S.L. Yan, Z. Sun, Y. Ying, B.K. Wang, Y.X. Tu, Depletion of HDAC1, 7 and 8 by histone deacetylase inhibition confers elimination of pancreatic cancer stem cells in combination with gemcitabine, Sci. Rep. 8 (2018) 1621.
[58] F.S. Giudice, D.S. Pinto Jr., J.E. Nor, C.H. Squarize, R.M. Castilho, Inhibition of histone deacetylase impacts cancer stem cells and induces epithelial-mesenchyme transition of head and neck cancer, PLoS One 8 (2013) e58672.
[59] M. Milanovic, D.N.Y. Fan, D. Belenki, J.H.M. Dabritz, Z. Zhao, Y. Yu, J.R. Dorr, L. Dimitrova, D. Lenze, I.A. Monteiro Barbosa, M.A. Mendoza-Parra, T. Kanashova, M. Metzner, K. Pardon, M. Reimann, A. Trumpp, B. Dorken, J. Zuber, H. Gronemeyer, M. Hummel, G. Dittmar, S. Lee, C.A. Schmitt, Senescence-associated reprogramming promotes cancer stemness, Nature 553 (2018) 96–100.